Developmental Cell, Volume *38*

Supplemental Information

PRG-1 Regulates Synaptic Plasticity via Intracellular PP2A/β1-Integrin Signaling

Xingfeng Liu, Jisen Huai, Heiko Endle, Leslie Schlüter, Wei Fan, Yunbo Li, Sebastian Richers, Hajime Yurugi, Krishnaraj Rajalingam, Haichao Ji, Hong Cheng, Benjamin Rister, Guilherme Horta, Jan Baumgart, Hendrik Berger, Gregor Laube, Ulrich Schmitt, Michael J. Schmeisser, Tobias M. Boeckers, Stefan Tenzer, Andreas Vlachos, Thomas Deller, Robert Nitsch, and Johannes Vogt

Supplemental Figure S1 to Figure 1

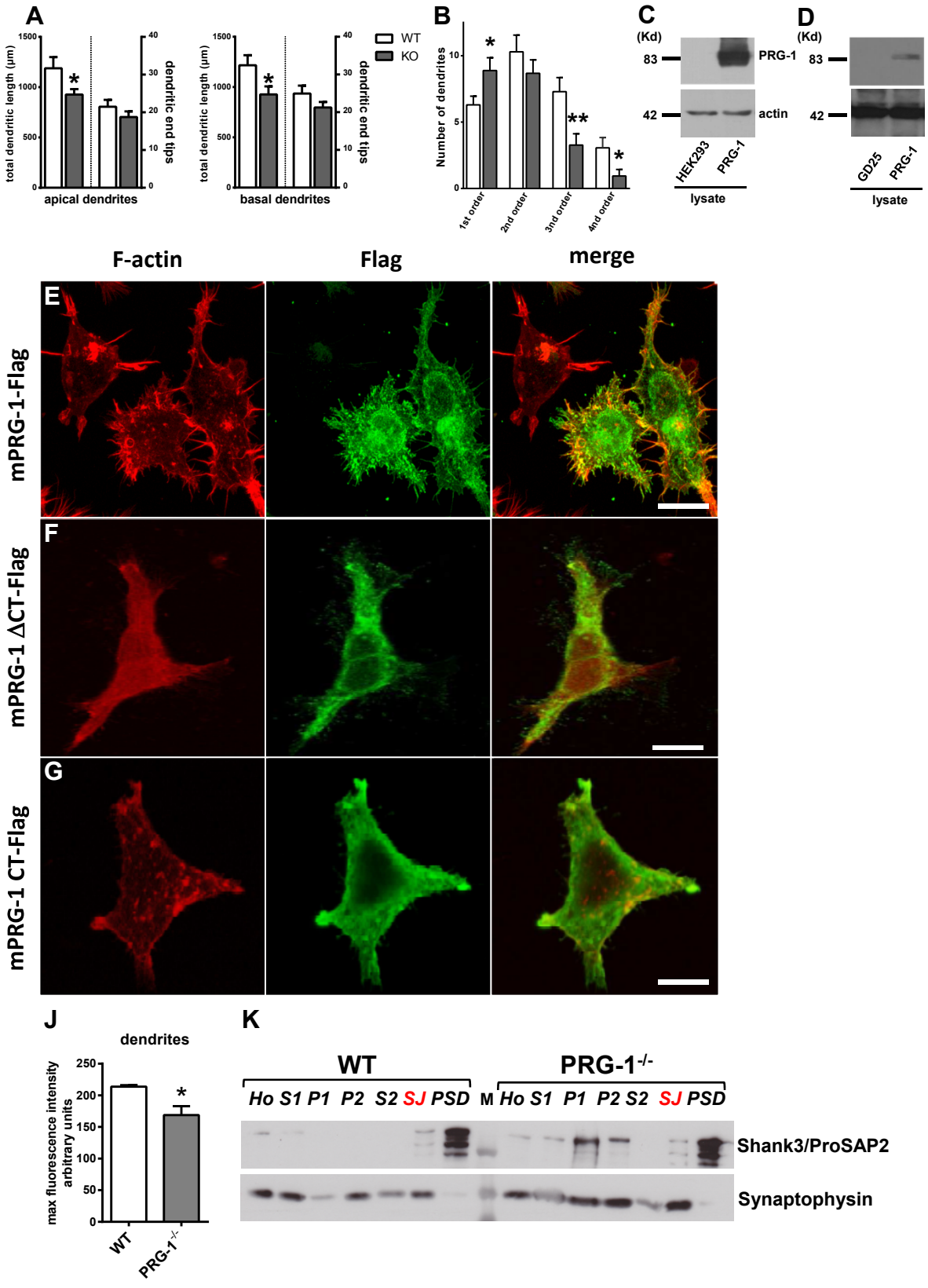

Supplemental Figure S2 to Figure 2

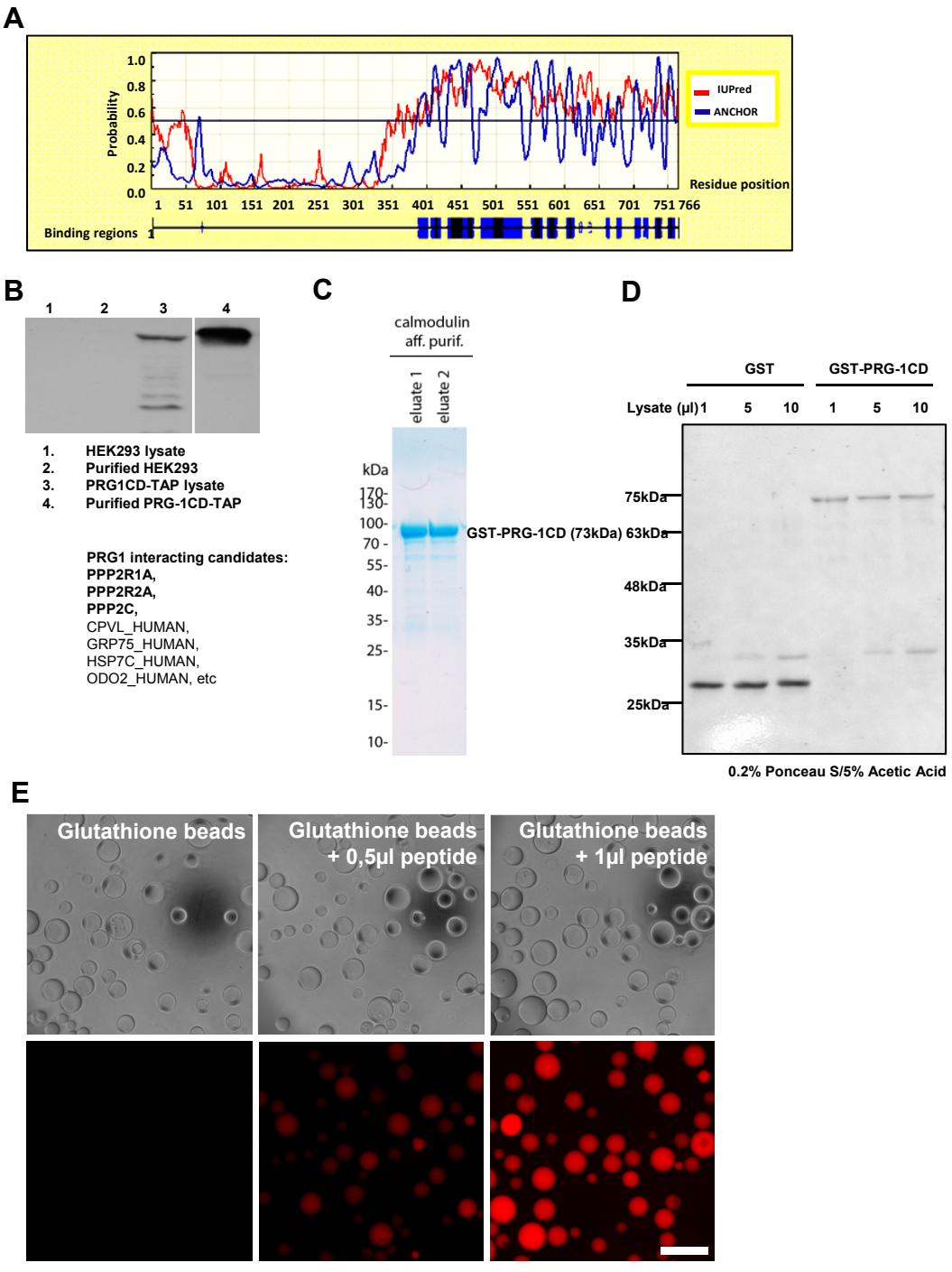

Supplemental Figure S3 to Figure 4

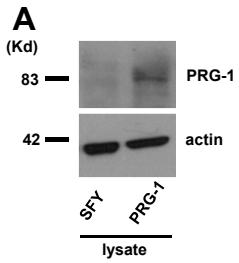

Supplemental Figure S4 to Figure 5

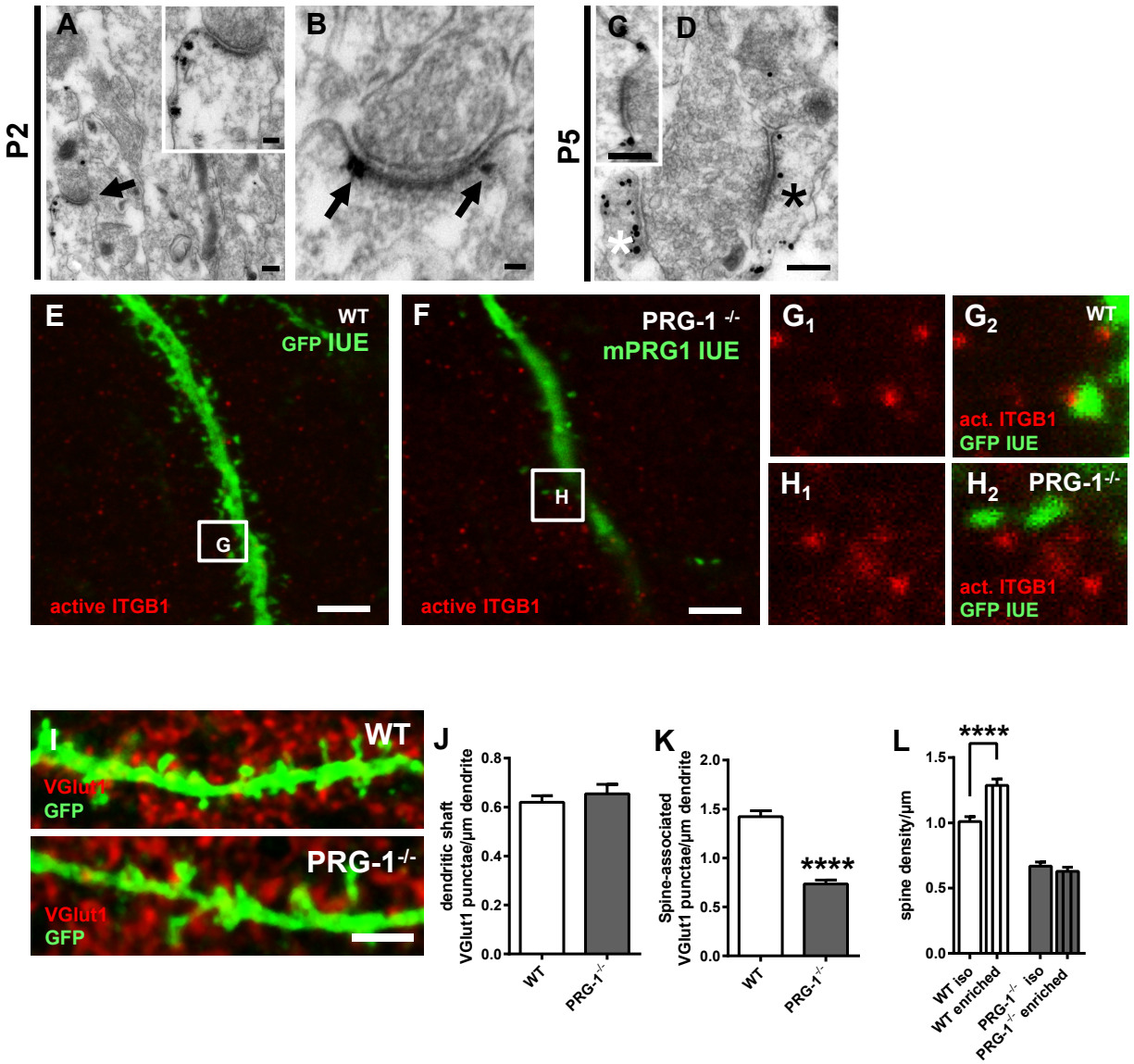

Supplemental Figure S5 to Figures 2-5

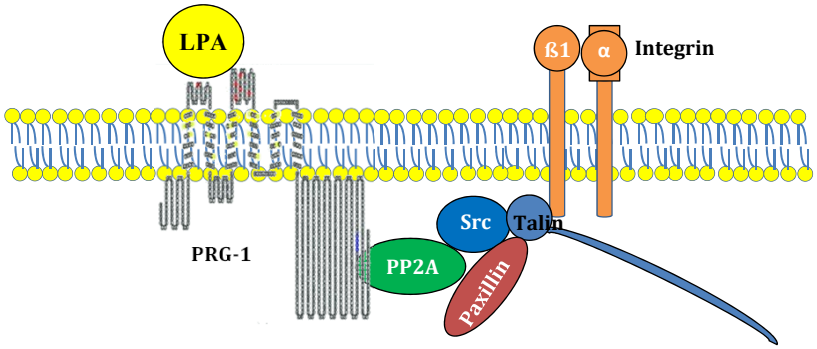

Supplemental Figure Legends

Supplemental Figure S1 related to Fig 1.

(A) Dendritic length in the apical and the basal dendrites of PRG-1$^{-/-}$ neurons is significantly reduced while and the number of dendritic end tips is not altered (n=17 WT and 19 PRG-1$^{-/-}$ neurons; Mann-Whitney test was performed for analysis of apical dendritic length and t-test were performed for all other comparisons).

(B) Dendritic arborization as assessed by comparison of number of dendritic segments of different order is significantly altered in PRG-1$^{-/-}$ neurons (n=17 WT and 19 PRG-1$^{-/-}$ neurons; t-test).

(C,D) Western blots demonstrating lack of PRG-1 in HEK-293 (C) and GD25 cells (D), and overexpression of PRG-1 in theses cell lines, respectively.

(E) HEK-293 cells display numerous actin containing filopodia upon full length PRG-1 transfection. PRG-1 is visualized via a fused Flag-tag (PRG-1-Flag fusion protein).

(F,G) HEK-293 cells expressing either a truncated PRG-1 (F), missing the intracellular C-term (mPRG-1ΔCT-Flag), or expressing only the intracellular C-term of PRG-1 (G, mPRG-1 CT-Flag), did not display filopodia. Scale bar E-G: 20 µm.

(J) Analysis of maximal fluorescence intensity of active ITGB1 signal revealed a decrease in PRG-1$^{-/-}$ neurons.

(K) Western blot of different steps of the Synaptic junction (SJ) preparation. Note the present synaptophysin (presynaptic marker) and the Shank3/ProSAP2 (postsynaptic marker; (Baron et al., 2006)) signal in the SJ fraction pointing to the presence of the presynaptic and the postsynaptic compartments in this fraction.

Supplemental Figure S2 related to Fig 2.

(A) Flexibility analysis of PRG-1 demonstrates high probability of PRG-1 cytoplasmic domain to bind with other molecules.

(B) Purification of intracellular C-terminal PRG-1 domain (PRG-1CD-TAP) according to standard procedures (Agilent technologies) and UPLC-MS analysis of the PRG1 interactome revealed novel PRG1 interacting candidates.

(C) Coomassie staining of the purified fusion construct of GST and PRG-1 C-terminal domain (GST-PRG-1CD) used for pulldown experiments. After glutathione affinity purification, GST-PRG-1CD was affinity purified using its described calmodulin interaction (Tokumitsu et al., 2010). The faint other remaining bands appear to result from degradation of the PRG-1 C-terminal domain, because they are exclusively between the sizes of the full length fusion

construct and GST alone. Furthermore GST containing fragments were detected by WB in this region (Fig. 2E).

(D) Ponceau S staining after protein transfer of pulldown product from SDS-PAGE to nitrocellulose membrane which was subsequently used for WB. After in vitro production of PPP2R2A, 1, 5 and 10 µl of the resulting lysate were used for pulldown experiment as indicated.

(E) Brightfield images (upper row) of glutathione beads incubated with different concentrations of the TAMRA-tagged PRG-1-554-588 peptide. Fluorescent images (lower row) showing the TAMRA-tagged PRG-1-554-588 peptide immobilized on glutathione beads. The different fluorescence intensities reflect the different concentrations of the peptide immobilized to glutathione beads. Control beads are devoid any fluorescence. Scale bar: 250 µm.

Supplemental Figure S3 related to Fig 4.

(A) Western Blot demonstrating lack of PRG-1 in SFY cells, and overexpression of PRG-1 in this cell line.

Supplemental Figure S4 related to Fig 5.

(A) PRG-1 expression was already found at P2, when CA1 neurons start to form first synapses. Insert shows a magnification of the stubby spine synapse shown in A.

(B) In more mature synapses found at this age, PRG-1, as shown by gold particles, is already expressed at the postsynaptic density of glutamatergic synapses and displays a similar expression pattern as revealed at adult ages.

(C,D) At P5, PRG-1 expression in CA1 neurons was observed at different stages of synapse formation: in dendritic filopodia contacting presynaptic terminals but not yet forming mature synaptic contacts (white asterisk), in stubby spines as shown in C, or in typical spines displaying PRG-1 expression at the postsynaptic density (black asterisk).

(E) Active ITGB1-staining in an in-utero *GFP* electroporated wildtype (wt) mouse displays clear punctae in the stratum radiatum (SR) of the hippocampal CA1 region.

(F) Image of in an in-utero GFP electroporated wildtype (PRG-$1^{-/-}$) mouse displays confirms lower spine density.

($G_{1,2}$) Higher magnification of the boxed area in the wt SR confirmed active ITGB1-expression at the tip of dendritic spines.

($H_{1,2}$) Higher magnification of the boxed area in the PRG-1$^{-/-}$ SR shows that active ITGB1-expression was not confined to dendritic spines.

(I) VGlut1-staining showing glutamatergic presynaptic terminals along a GFP-expressing dendritic segment (Thy-1 L21 line) in a WT and in a PRG-1$^{-/-}$ animal.

(J) Quantitative assessment of dendritic associated VGlut1-punctae revealed no difference between WT and PRG-1$^{-/-}$ animals (n=51 WT dendritic segments and 49 PRG-1$^{-/-}$ dendritic segments, unpaired t-test).

(K) Spine-associated VGlut-1 punctae revealed a significant decrease in PRG-1$^{-/-}$ mice which is in line with reduced spine densities found in these animals (n=51 WT dendritic segments and 49 PRG-1$^{-/-}$ dendritic segments, unpaired t-test).

(L) Spine density was significantly increased in WT animals kept under enriched conditions when compared to those kept in isolation. In contrast, in PRG-1$^{-/-}$ animals, dynamic regulation of spine density under enriched conditions was aborted and remained at the same low levels as observed in PRG-1$^{-/-}$ animals kept under isolation conditions.

Scale Bars: A: 200nm, insert: 80nm ;B: 40nm; C,D: 200nm; E,F: 5 µm, I: 4µm.

Supplemental Figure S5 related to Figures 2-5.

Schematic diagram of the signaling pathway analyzed.

Supplemental Experimental Procedures

Isolation, culture and analysis of hippocampal neurons

Primary hippocampal neurons from embryonic day 17 (E17) pregnant mice were prepared as previously described (Vogt et al., 2012). Briefly, after brain dissection and trypsin digestion, 10^5 neurons triturated using fire polished glass pipets were seeded on GG-18-fibronectin (neuVitro) or poly-l-lysine coated coverslips in Minimum Essential Medium (Gibco) supplemented with 10% Horse Serum, 100 U/ml penicillin and 100 µg/ml streptomycin (Gibco), 0.6% Glucose (Fresenius Kabi) and kept at 37 °C/5% CO_2. After 3 h, neurons were washed once with pre-warmed PBS, and incubated with Neurobasal Medium (Gibco) supplemented with 2% B-27, 100 units/ml penicillin, 100 µg/ml streptomycin and 0.5 mM glutamine (Gibco). For analyses, neurons were either 1. transfected at days in vitro 8 (DIV) with pEGFP-N1 or pEGFP-N1 combined with *pPRG-1-FLAG* (1:1) and analyzed at DIV14 or 2. treated with FTY720 (100 nM) starting at DIV6, transfected at DIV10 with a pCAG-IRES-EGFP vector (Kawauchi et al., 2003) and analyzed at DIV12 or 3. transfected at DIV 8, treated for 24 h with 1 nM Okadaic acid (OA) at DIV9 and analyzed at DIV10. Neurons were subsequently fixed with 4% paraformaldehyde, permeabilized, blocked with PBS containing 0.2% Triton X-100 and 5% goat serum (Vector Laboratories) and incubated with one or a combination of the following primary antibodies: mouse monoclonal anti-FLAG (M2, 1:1000, Sigma), rat monoclonal anti-active integrin ß1 (ITGB1, 9EG7, 1:200, BD Biosciences), rat anti-ITGB1 (1:200, MAB2405, R&D Systems), mouse anti-PSD95 (Synaptic Systems), rabbit anti-PRG-1 (1:2500 custom-made antibody against aa 624-637, NP_808332 as described by (Trimbuch et al., 2009)) or rabbit anti-GFP (1:1000, Abcam).

Light microscopy and Sholl analysis.

pEGFP-N1 transfected neurons were converted after fixation with diaminobenzidine (DAB) using a GFP-antibody (abcam) and a biotinylated secondary antibody (Vector Laboratories). DAB labeled neurons from WT and PRG1-KO were analysed by transmitted light microscopy. Images were taken using an upright Zeiss microscope and a 20x objective (numerical aperture 0.6). Analyses were done with the software ImageJ. By using Sholl analysis (Sholl, 1953) we could quantify the number of dendritic intersections of a neuron with cross concentric circles (from 50 µm to 350 µm diameter). Furthermore we measured total dendritic length on both apical and basal dendrites and determined the branchpoints of higher order dendrites.

Quantitative analysis of neurons

Neurons were imaged with a Leica SL or a Leica TCS SP8 confocal laser scanning microscope equipped with a white light laser (WLL) using identical laser power settings and acquisition properties for the compared conditions. Spine analysis, analysis of total and active ITGB1 expression in cell bodies and dendritic segments, respectively, were performed by an experimenter blinded to the experimental conditions using ImageJ. Mean fluorescence was quantified as grey value along dendritic segments using ImageJ. Total length of dendritic segments assessed was at least 900 µm per condition. To ensure that the analysis was not confounded by the presence of clusters of activated ITGB1 in PRG-1$^{-/-}$ neurons that contain higher amounts of active ITGB1 as in controls, clusters of active ITB1 in PRG-1$^{-/-}$ neurons were assessed in their maximal pixel grey value with those of wt neurons (Supplemental Fig. S1J).

For delineation of the corresponding ROIs using the free hand selection tool in ImageJ, images were (over-)enhanced in brightness and contrast using ImageJ, allowing for determination of dendritic segments. ROIs were then transferred to the original image and measures were performed using ImageJ. For assessment of active ITGB1 expression in PSD95 punctae on the dendritic shaft, images were thresholded using background values and ROIs were detected using the "analyse particle" function of ImageJ. To avoid for bias by unspecific recognition, only particles bigger than 0.025 µm^2 (10 pixel size) were taken into account. ROIs were then transferred to original images and mean values were measured using ImageJ. In order to compare values for different experimental conditions, all values were calculated in percent of the corresponding WT values.

Fluorescence microscopy spine and dendritic synapse quantification.

GFP positive brain slices and fluorescently labeled cell culture neurons were imaged with a Leica confocal laser-scanning microscope (SL or SP8). Single cell overview images were done with a 40x oil objective (numerical aperture 1.25). For spine measurement a 63x oil objective (numerical aperture 1.4; optical zoom 4 or zoom 5) was used for z-series stacks with a step size of 0.2µm. Fluorescent images were quantified using ImageJ. Spines were defined as dendritic protrusions from 0.5µm up to 5µm in length and were manually counted along a selected dendritic segment using ImageJ. In brain slices we focus our analyses on three populations of dendrites: (1) the dendrites within the middle molecular layer of granule cells; (2) stratum radiatum and (3) stratum oriens of pyramidal neurons of the CA1 region. Analysis of dendritic and spine synapses was performed in the CA1 region. For each genotype and age around 1000 spines or at least 1000 µm dendritic length were measured,

dependent which condition was fulfilled first. For each dendritic segment the number of spines per µm dendrite was calculated and data from one group were averaged.

Long-term potentiation (LTP)

Mice (16-18 day-old mice for data shown in Fig.1F or adult mice either untreated or treated over 30 days with 5 mg/kg FTY720 body weight/day (controls were treated in the same way using the solvent) for data shown in Fig. 3L,M, Fig. 5L) were anesthetized with isoflurane and rapidly decapitated. Experiments were performed as previously described (Fan, 2013). Transverse slices (400 µm) were prepared using a vibratome (Leica VT1200S) and immersed in ice cold artificial cerebrospinal fluid (ACSF) containing 126 mM NaCl, 2.5 mM KCl, 1.25 mM NaH_2PO_4, 1 mM $MgCl_2$, 2 mM $CaCl_2$, 26 mM $NaHCO_3$ and 10 mM D-glucose (saturated with 95% O_2 and 5% CO_2). Slices were incubated at 32 °C for at least 1 h before transfer to a submersion-type chamber for recording. Slices were allowed to recover for 30 min in the recording chamber after positioning of recording and stimulating electrodes. Field excitatory postsynaptic potentials (fEPSPs) in CA1 stratum radiatum were evoked by stimulation of Schaffer-collateral fibers with biphasic constant pulses (0.2 ms/polarity) at 0.033 Hz. fEPSPs were recorded at 30-40% of the maximum amplitude obtained in an input-output curve test. In Fig. 1F, long-term potentiation (LTP) was induced with high frequency stimulation (HFS) consisting 3 trains of 100 stimuli at 100 Hz, 10 min inter-train interval. In Fig. 3L,M and Fig 5L, LTP was induced with theta-burst stimulation (TBS): 3 trains of 10 bursts at 5 Hz, with each burst consisting 4 stimuli at 100 Hz, 30 s inter-train interval. Data were recorded every 30 sec and was averaged in 5 min bins. In order to avoid bias by outlier values, outlier analysis was performed using GraphPad Prism 6 (Version 6.07) using the ROUT method which is able to identify multiple outliers.

DNA constructs

Mouse *PRG-1* and human *ITGB1* cDNAs were amplified by One-Step RT-PCR Kit (Roche) using mRNA from mouse cortex or HEK-293 cells as template respectively. *PRG-1* coding sequence was cloned into pIRESneo3 (Clontech) between NheI and BamHI to get pIRESneo3-PRG-1; *PRG-1CD* (PRG-1 cytoplasmic C-terminal domain) coding sequence was cloned into pNTAPB (Stratagene) between BamHI and ApaI restriction sites to get pNTAPB-PRG-1CD; Human *ITGB1* coding sequence was cloned into pIRESpuro3 (Clontech) between NheI and BamHI to get pIRESpuro3-hITGB1. Truncated form of *PRG1* coding for amino acids 554 to 588 (CaM binding domain), was prepared by using QuickChangeII XL Site-Directed Mutagenesis Kit (Stratagene) using pIRESneo3-PRG1 as

template plasmid. *Src* cDNA was from Addgene and subcloned into pIREShyg3 between NheI and BamHI. The plasmids pCAG-mPRG-1 and pCAG-cre were constructed by inserting the corresponding coding frame into the multiple cloning site (MCS) of a pCAG-IRES-eGFP vector (Kawauchi et al., 2003). pPRG1-FLAG was prepared using pEGFP-N1 (Stratagene) as backbone, its EGFP coding sequence was replaced by FLAG sequence from p3xFLAG-CMV (Sigma) and PRG-1 reading frame or its mutated forms were inserted between EcoRI and BamHI. R345T mutant of PRG-1 (*PRG-1*^{R345T}) was constructed as described (Vogt et al., 2016). Insertion of DNA coding the C-terminal cytoplasmic domain of murine *PRG-1* (amino acids 338-766) into the vector pGEX-6P-1 (GE Healthcare) between the BamHI and NotI restriction sites using standard cloning techniques resulted the plasmid for bacterial production of a GST-PRG-1CD fusion protein.

Cell culture, transfection, cell line establishment and immunocytochemistry

HEK-293, GD25 (provided by Reinhard Faessler) and MEF-SFY (provided by Mirko Schmidt) cell lines were cultured in DMEM (Gibco) supplemented with 10% fetal bovine serum (Pan-Biotech), 100 U/ml penicillin, 100 µg/ml streptomycin, 2 mM L-glutamine and 0.1 mM MEM non-essential amino acids (all from Gibco) at 37 °C / 5% CO_2. Stable cell lines were established by continual application of G418 (600 µg/ml), hygromycin (50 µg/ml) or puromycin (0.5 µg/ml) in complete DMEM after calcium phosphate or lipofectamine 2000 (invitrogen) transfection, and followed by picking and amplifying antibiotics resistant clones according to standard protocol. The selected and amplified cell clones were maintained in complete DMEM containing corresponding antibiotics at half the concentrations for selection. Introduction of DNA for transient expression of exogenous genes was carried out using classical calcium phosphate or lipofectamine (ThermoFisher Scientific) methods on HEK-293 and GD25 cells. For immunostaining, cells were fixed with 4% paraformaldehyde, permeabilized, blocked with PBS containing 0.2% Triton X-100 and 5% goat serum (Vector Laboratories) or 10% FCS and incubated mouse monoclonal anti-Vinculin (SPM227, 1:200, abcam), mouse monoclonal anti-FLAG (M2, 1:1000, Sigma), Phalloidin (Sigma) and subsequently visualized with a secondary goat anti mouse antibody conjugated to Alexa Fluor 546 or to Alexa Fluor 488 (1:1000, Invitrogen). Confocal imaging was performed as described above.

Cell adhesion assay

Cell adhesion was assayed as described in instruction manual of ECM Cell Adhesion Array Kit (Chemicon) with little modification. Briefly, cells at log phase were starved for 24h, then detached from the dishes using 2 mM EDTA in DPBS-CMF (Dulbecco's phosphate-buffered

saline without calcium and magnesium, Gibco) and collected. Single cell suspensions were prepared in HBSS-CMF (Hanks buffered salts solution without calcium and magnesium) supplemented with 0.1**%** fatty acid free BSA (Albumin bovine fraction V) (SERVA) and 25 mM HEPES to achieve 1.0 x 10^6 cells/ml, 100 µl cells (1x 10^5 cells) were seeded in each well of the ECM array plate or fibronectin or laminin coated strips (Chemicon) having been rehydrated with DPBS-CMF for 10 min at room temperature. After 2 h incubation at 37 °C and 5% CO_2, non-adherent cells were removed by washing 3 times with DPBS-CMF, whereas 100 µl of Cell Stain Solution (Chemicon) per well were added to the remaining adherent cells and incubated for 5 min at room temperature. After staining the wells were washed 3 to 5 times with deionized water and then air dried. Random fields from each well were taken for images (10x magnification) and the number of adherent cells was counted, or the cell-bound stain was solubilized by 100 µl Extraction Buffer (Chemicon) and measured at 540-570 nm on a microplate reader. For cell adhesion inhibition assays cells were preincubated with the following drugs respectively: 100 nM Echistatin (Sigma) for 1 h, 2 µg/ml anti-ITGB1 (P5D2, abcam), 1 µM LPA (Enzo Life Sciences) added just before adherent, 1 µg/ml FTY720 (Sigma) for 1 h, 100 nM Okadaic acid (Biomol) for 2 h, 1 µM PP2 (Sigma) for 1 h, 5 mM Methyl-ß-cyclodextrin (MßCD), 25 µg/ml Nystatin (Sigma) for 30 min.

Flow cytometry

All flow cytometry analyses were carried out on a FACS Canto II cytometer (BD Biosciences). To analyze ITGB1 activation, HEK-293 cell lines expressing PRG-1 and HEK-293 cells were cultured till around 80% confluent, washed twice with DMEM without phenol red indicator to get rid of dead cells, harvested, resuspended in DMEM and filtered through cell strainer for further use. One million cells were preincubated at 4 °C for 10 min with 5 µg human IgG (Sigma) to block Fc receptors, then incubated with 5 µg FITC-conjugated ITGB1 antibody (TDM29/CBL481, Millipore) for total surface ITGB1 staining or antibody to activated ITGB1 (HUTS-4, Millipore) followed by Alexa 488-conjugated F(ab´)2 fragment of rabbit anti-mouse IgG (1:2000, Invitrogen) staining. Integrin activation status was also analyzed by its echistatin affinity. For this aim, one million cells were firstly incubated with 100 nM echistatin (sigma), then incubated with 5 µg rabbit anti-echistatin antibody (Millipore) and subsequently with Alexa 488-conjugated F(ab´)2 fragment of goat anti-rabbit IgG (1:2000, Invitrogen). For intracellular talin staining, one million prepared single cell suspension was fixed with ice cold methanol and permeabilized by 0.1% Triton X-100, then incubated with talin rod domain (8D4), talin pS425 (ECM Bioscience) or talin head domain (TA205, Sigma), followed by Alexa 488-conjugated F(ab´)2 fragment of rabbit anti-mouse or goat anti-rabbit IgG (1:2000, Invitrogen).

Synaptic junction (SJ) preparation

SJ fraction was isolated as recently described (Distler et al., 2014). The animal experiments were conducted in accordance with national laws and approved by the local authorities. Subcellular fractionation was performed from six independent samples. Each sample contained hippocampi pooled from 10-11 mice. All buffers were supplemented with protease and phosphatase inhibitor mix (Roche) and all steps were either performed at 4 °C or on ice. Briefly, tissue was homogenized in buffer (320 mM sucrose, 5 mM HEPES, pH 7.4) using a teflon douncer. The homogenate (Ho) was centrifuged for 10 min at 1,000 x g to remove cell debris and nuclei (P1). The supernatant (S1) was further centrifuged for 20 min at 12,000 x g to obtain the soluble fraction (S2) and the crude synaptosomes (P2). P2 was resuspended in a Tris buffer (320 mM sucrose, 5 mM Tris/HCl, pH 8.1) and centrifuged in a sucrose density gradient (0.8 M/1.0 M/1.2 M) for 2 h at 200,000 x g. Purified synaptosomes were collected from the 1.0/1.2 interphase, diluted in five volumes of 1 mM Tris/HCl, pH 8.1, lysed for 30 min by stirring and centrifuged for another 30 min at 33,000 x g. The resulting pellet was resuspended in 5 mM Tris/HCl, pH 8.1, and centrifuged in another sucrose density gradient (0.8 M/1.0 M/1.2 M) for 2 h at 200,000 x g for additional purification. Synaptic junctions (SJ) were collected from the 1.0/1.2 interphase, subsequently resuspended in Tris buffer containing 0.5% Triton X-100, stirred for 15 min and centrifuged for another 30 min at 33,000 x g to obtain a one-Triton extracted PSD fraction (PSD). For characterization of the PSD-preparation an antibody against Shank3 (described in (Schmeisser et al., 2012)) and an antibody against Synaptophysin (Abcam) were used.

Western Blotting (WB)

WB was performed according to standard procedures. Briefly, samples were separated by SDS-PAGE using 10% polyacrylamide gels, and blotted on a nitrocellulose membrane (0.45 µm; BIO-RAD, USA) by semi-dry transfer cell (BIO-RAD, USA) at 100 mA for 40 min. Blots were blocked overnight at 4 °C in 10% non-fat dry milk, washed twice, and incubated at room temperature (RT) for 3 h with corresponding antibodies in 1% non-fat BSA. After three washes, membranes were incubated with a corresponding horseradish peroxidase-conjugated antibody (1:5000 dilution; dianova, Germany) in 1% non-fat BSA at RT for 1 h. Immunoreactive bands were detected using SuperSignal West Femto Maximum Sensitivity Substrate kit (Thermo Scientific, USA) according to standard protocols. Quantification of immunosignals was performed using ImageJ.

Preparation of the PRG-1CD interactome

Cell lines expressing PRG-1CD fusion protein with tandem streptavidin binding peptide (SBP) and calmodulin binding peptide (CBP) tags at N terminus were established as above and pull-down assays were carried out according to instruction manual of InterPlay® Mammalian TAP System (Agilent technologies). Tandem affinity purification (TAP) pulldown and control eluates were lyophilized and resolubilized in lysis buffer (7M Urea, 2M ThioUrea, 2% Chaps). Subsequently, proteins were digested using a modified filter-aided sample preparation (FASP, (Wisniewski et al., 2009)). Briefly, redissolved protein was loaded on the filter, and detergents were removed by washing three times with buffer containing 8 M urea. The proteins were then reduced using DTT, alkylated using iodoacetamide, and the excess reagent was quenched by addition of additional DTT and washed through the filters. Buffer was exchanged by washing with 50 mM NH_4HCO_3 and proteins digested overnight by trypsin (Trypsin Gold, Promega) with an enzyme to protein ratio of 1:50. After overnight digestion, peptides were recovered by centrifugation and two additional washes using 50 mM NH_4HCO_3. Flowthroughs were combined, lyophilized and redissolved in 20 µl 0.1% formic acid by sonification. The resulting tryptic digest solutions were diluted with aqueous 0.1% v/v formic acid to a concentration of 200 ng/µl and spiked with 25 fmol/µl of enolase 1 (*Saccharomyces cerevisiae*) tryptic digest standard (Waters Corporation).

UPLC-MS configuration

Nanoscale LC separation of tryptic peptides was performed with a nanoAcquity system (Waters Corporation) equipped with a HSS-T3 C18 1.8 µm, 75 µm x 250 mm analytical reversed-phase column (Waters Corporation) in direct injection mode as described before (Tenzer et al., 2011)). 0.2 µl of sample (40 ng of total protein) was injected per technical replicate. Mobile phase A was water containing 0.1% v/v formic acid, while mobile phase B was ACN containing 0.1% v/v formic acid. Peptides were separated with a gradient of 3–40% mobile phase B over 120 min at a flow rate of 300 nl/min, followed by a 10-min column rinse with 90% of mobile phase B. The columns were re-equilibrated at initial conditions for 15 min. The analytical column temperature was maintained at 55 °C. The lock mass compound, [Glu^1]-Fibrinopeptide B (100 fmol/µL), was delivered by the auxiliary pump of the LC system at 300 nl/min to the reference sprayer of the NanoLockSpray source of the mass spectrometer. Mass spectrometric analysis of tryptic peptides was performed using a Synapt G2-S mass spectrometer (Waters Corporation, Manchester, UK). For all measurements, the mass spectrometer was operated in v-mode with a typical resolution of at least 25 000 FWHM (full width half maximum). All analyses were performed in positive mode ESI. The time of flight analyzer of the mass spectrometer was externally calibrated with a NaI mixture

from **m/z** 50 to 1990. The data were post-acquisition lock mass corrected using the doubly charged monoisotopic ion of [Glu[1]]-Fibrinopeptide B. The reference sprayer was sampled with a frequency of 30 s. Accurate mass LC-MS data were collected in data-independent modes of analysis (Geromanos et al., 2009) (Silva et al., 2005) in combination with on-line ion mobility separations. For ion mobility separation, a wave height of 40 V was applied. Traveling wave velocity was ramped from 800 m/s to 500 m/s over the full IMS cycle. The spectral acquisition time in each mode was 0.7 s with a 0.05 s interscan delay. In low energy MS mode, data were collected at constant collision energy of 4 eV. In elevated energy MS mode, the collision energy was ramped from 25 to 55 eV during each 0.7 s integration. One cycle of low and elevated energy data was acquired every 1.5 s. The radio frequency (RF) amplitude applied to the quadrupole mass analyzer was adjusted such that ions from **m/z** 350 to 2000 were efficiently transmitted, ensuring that any ions observed in the LC-MS data less than **m/z** 350 were known to arise from dissociations in the collision cell. All samples were analyzed in triplicate.

UPLC-MS data processing, protein identification and statistical analysis

Continuum LC-MS data were processed and searched using ProteinLynx GlobalSERVER version 2.5.2 (Waters Corporation). The resulting peptide and protein identifications were evaluated by the software using statistical models as described (Tenzer et al., 2011). Protein identifications were assigned by searching the mouse taxon of the *UniProtKB/SwissProt* database (release 2012_01) supplemented with known possible contaminants and standard proteins (porcine trypsin, yeast enolase, BirA, streptavidin) using the precursor and fragmentation data afforded by the LC-MS acquisition method as reported (Tenzer et al., 2011). The search parameter values for each precursor and associated fragment ions were automatically set by the software using the measured mass error obtained from processing the raw continuum data. Peptide identifications were restricted to tryptic peptides with no more than one missed cleavage. Carbamidomethyl cysteine was set as fixed modification, and oxidized methionine, protein N-acetylation, and deamidation of asparagine and glutamine were searched as variable modifications. Database search was performed allowing a maximal mass deviation of 3 ppm for precursor ions and 10 ppm for fragment ions. For valid protein identification, the following criteria had to be met: at least 2 peptides were detected with together at least 7 fragments. All reported peptide identifications provided by the IDENTITY^{E}-algorithm are correct with >95% probability as described (Tenzer et al., 2011). The initial false positive rate for protein identification was set to 3% based on search of a 5x randomized database, which was generated automatically using PLGS2.5.2 by randomizing the sequence of each entry. By using replication rate of identification as a filter,

the false positive rate is further reduced to <0.1%. Additional data processing including retention time alignment, normalization, isoform/homology and replicate filtering, as well as final TOP3 based label-free quantification was performed using the ISOQuant software pipeline as described previously (Patzig et al., 2011).

Bioinformatics and statistical analysis. Hierarchal clustering analysis was performed based on absolute label-free protein quantification results provided by ISOQuant using dedicated *R* scripts in *R2.14.0* execution environment (Tenzer et al., 2011).

Immunoprecipitation and immunoblotting

HEK-293 cells expressing PRG-1 or mechanically homogenized cortex tissue were lysed in appropriate volume of lysis buffer (50 mM Tris-HCl pH 7.4, 1% Triton X-100, 1% n-Octyl ß-D-glucopyranoside, 0.1% SDS, 1 mM EDTA pH7.0, 150 mM NaCl) containing protease inhibitors (Roche) for 1 h on ice, and cleared by centrifugation for 10 min at 15000 g at 4 °C. The following lysate preclearing with agarose slurry, incubation with PRG-1 antibody (1:100), or normal rabbit IgG (1:100, Millipore) as control, and pull-down by Protein G agarose resin (Thermo Scientific) were carried out according to standard protocols. The following primary antibodies was used for immunoblotting: PRG-1 (1:3000, custom-made antibody against aa 624-637, NP_808332) (Trimbuch et al., 2009). Following antibodies were used for immunoblotting: ITGB1, PPP2R1A (81G5), PPP2R2A (100C1), PPP2C (52F8), Src (32G6), Talin (C45F1), Paxillin pY118 (1:1000) all from Cell Signaling, Caveolin-1 (Cav1) (1:2000, Sigma), PPP2C pY307 (E155, 1:1000, abcam), ß-actin (1:5000, MP Biomedicals). For immunoblotting, cell lysates or immunoprecipitated samples were separated by SDS-PAGE and transferred onto nitrocellulose membrane (Bio-Rad). After incubation with first antibodies and HRPO-conjugated secondary antibodies (1:5000, dianova), membranes were developed by ECL (Amersham Biosciences) according to standard protocols.

Proximity Ligation Assay (PLA)

The following primary antibodies were used for PLA: PRG-1 (1:1000, custom-made antibody against aa 624-637, NP_808332) (Trimbuch et al., 2009)), PPP2R2A (2G9), Src (32G6), Paxillin (1:100), Cav1 (D46G3), HA-Tag (6E2,1:200) and FAK (1:200) all from Cell Signaling, PPP2C (1D6, 1:100), ITGB1 C terminus (EP1041Y, 1:250) from Millipore, PPP2R1A (4E6) and Talin (TA205) (1:100) from Sigma, FAK central region (M246, 1:200) from ECM Bioscience and Caveolin1 (7C8, 1:125) from Thermo Scientific. The in situ PLA was used to detect protein-protein interactions in fixed cells. PRG-1 expressing or HEK-293 cells or primary neurons were fixed with 4% PFA followed by blocking with blocking solution. Then

incubations with primary antibodies, with the PLA probes (anti-mouse and anti-rabbit IgG antibodies conjugated with oligonucleotides), ligation and amplification according to the user manual of Duolink® II Fluorescence (Olink® Bioscience). Imaging was performed on a Leica SP8 confocal laser scanning microscope. For the evaluation of the specific number of dots per cell, pictures of cells with positive PLA signal were used. Cell delineation was performed by adjusting the DAPI-signal. Quantitative analysis was performed either by counting PLA-positive dots per cell/cell in the visual field or by assessment of the fluorescence signal per cell as mean gray values using ImageJ.

Purification of GST-PRG-1CD

E. coli T7Express (NEB) cells transformed with pGEX-6P-1-GST-PRG-1CD grew over night on an LB-ampicillin agar plate at 37 °C. A single colony served for inoculation of a 100 mL LB-ampicillin overnight shaking culture at 37 °C. The next day 1 L 2xYT-ampicillin medium in a 2 L shaking flask was inoculated to an OD600 of 0.1 and incubated shaking at 37 °C till the OD600 reached 0.3 at which time the cooling to 30 °C started. At an OD600 of 0.6-0.8 addition of 0.2 mM IPTG induced protein production. Cells were harvested after 4 h, weighed, suspended in an equivalent amount of 20 mM HEPES buffer pH 7.5 and frozen in liquid nitrogen. For cell disruption 12 g frozen suspended cell pellet melted in a total final volume of 30 mL lysis buffer (50 mM HEPES pH 7.5, 2 mM $MgCl_2$, 1 g/L lysozyme, EDTA free protease inhibitor (Roche)). Afterwards stirring continued for 30 min at 4 °C. All following steps were performed on ice or at 4 °C. Six cycles of 30 s ultra-sonication (Branson Sonifier 250, duty cycle 70%, output 8) followed by 30 s cooling on ice disrupted the cells. 20 min centrifugation at 14000 rpm pelleted cell debris. The clarified supernatant was adjusted to 150 mM NaCl, filtered (0.45 µm) and batch loaded for 1 h on 1 mL glutathione superflow agarose resin (Pierce) equilibrated in wash buffer (20 mM HEPES pH 7.5, 150 mM NaCl). The settled loaded resin was transferred in a gravity flow column, washed with 12 mL washing buffer and the protein was eluted with 6 mL elution buffer (20 mM Tris pH 8, 150 mM NaCl, 10 mM reduced glutathione). The eluate was adjusted to 40 mM HEPES pH 7.5, 300 mM NaCl, 5 mM $CaCl_2$, 1 mM $MgCl_2$ and supplemented with 1x EDTA-free protease inhibitor in a final volume of 7 mL. To purifiy the GST-PRG-1CD via the native calmodulin binding of the PRG-1 domain the solution was batch loaded for 1 h on 0.5 mL calmodulin sepharose 4B resin (GE Healthcare) equilibrated in washing buffer (40mM HEPES pH 7.5, 2 mM $CaCl_2$, 300 mM NaCl, 1 mM imidazole). After washing the resin with 8 mL washing buffer the protein was eluted with elution buffer (40 mM HEPES pH 7.5, 2 mM EGTA, 300 mM NaCl). The first two 1 mL fractions containing most of the purified GST-PRG-1CD were pooled.

Pulldown with purified intracellular C-terminal domain PRG-1 (GST-PRG-1CD) in a cell-free system

The regulatory subunit PP2A beta subunit PPP2R2A was produced in a cell free – rabbit reticulolysate system (Promega, L1170) following manufacturer's instructions using a pCAG-*PPP2R2A* expressing construct as a template. In this approach, rabbit reticular lysates are treated with micrococcal nuclease destroying endogenous mRNA and thus preventing background translation. Due to its cell-free nature devoid of cellular membrane components, content of membrane proteins is reduced by large. The lysate from this PPP2R2A-producing system excludes, for the most part, putative intermediate interaction partners of PRG-1 which might mediate an indirect interaction with PP2A. For in-vitro interaction studies, 1 to 10 µl of lysate were mixed with 2 µg of GST (control) or GST coupled purified PRG-1CD protein, and 10 µl of glutathione-sepharose (GE healthcare) in 200 µl of binding buffer (25 mM Tris-HCl pH 7.2, 150 mM NaCl, 1% NP-40, 5 mM $MgCl_2$, and 5% glycerol). For specific interaction studies, 0.5 µl and 1 µl of a 1 mM peptide solution corresponding to PRG-1 aa 554-588 which was tagged to TAMRA as a fluorescence indicator dye was immobilized to 10 µl of glutathione-sepharose in 200 µl binding buffer. Subsequently 200 µl of binding buffer containing 1 µl of reticular lysate was added to the resin. Binding of PRG-1 aa 554-588 to glutathione-sepharose was determined by its fluorescence TAMRA tag. Control beads showed no fluorescence signal (Supplemental Fig. S2E). Fluorescent pictures were taken on an inverse microscope from DMi8 from Leica. All pictures were taken using same settings and were adjusted for brightness and contrast in the same way. After 2 h of incubation at 4 ˚C, the resin was washed twice with ice cold binding buffer. The samples were used for 10% acrylamide gel SDS-PAGE followed by western blotting analysis on nitrocellulose membrane. PPP2R2A was detected on the membrane after blocking with 3% BSA/TBST (20mM Tris-HCl pH 7.5, 150 mM NaCl, and 0.05% Tween-20) by an anti-PP2A beta subunit antibody (Cell Signaling, 100C1 #2290) and a HRP conjugated anti-rabbit antibody (NOVEX, A16096). GST coupled protein was detected by anti-GST antibody (Santa Cruz, SC-138) and HRP conjugated anti-mouse IgG (GE healthcare, NA9310-1ML).

Lipid raft preparation

Lipid rafts were extracted according to instruction manual of Caveolae/Rafts Isolation Kit (Sigma). Briefly, for each density gradient one 10 cm dish of cells (80% confluent) were lysed with 1 ml lysis buffer containing 1% Triton X-100, OptiPrep density gradient was prepared and centrifuged at 200,000 g using SW 40 Ti rotor (Beckman) for 4 h at 4 °C. From top to bottom of the ultracentrifuge 1 ml fractions were carefully collected and transferred to a marked microcentrifuge tube.

Serine/Threonine Phosphatase Assay

For serine/threonine phosphatase assay, the elute samples were prepared according to instruction manual of InterPlay® Mammalian TAP System (Agilent technologies) from pNTAPB-PRG-1CD transfected cells and HEK-293 cells as control. Additionally, we also tested phosphatase activity in lysates. For this aim pNTAPB-PRG-1CD transfected and control cells were firstly lysed in appropriate volume of lysis buffer, freeze-thaw cycles for 3 times and cleared by centrifuge for 10 min at 15000 g at 4 °C. Then the free phosphates were removed from samples by Sephadex® G-25 resin before phosphatase assay was carried out following instructions of Serine/Threonine Phosphatase Assay System (Promega).

Transgenic animals and breeding.

Constitutive and conditional PRG-1-KO mice were used. For generation of the mice and genotyping see Trimbuch et al. (2009). To visualize the neurons, particularly the dendrites and the dendritc spines, PRG-$1^{+/-}$ animals of the constitutive mouse line were bred with Thy-1.2-EGFP_L21 mice (Caroni, 1997). To generate a PRG-$1^{-/-}$/LPA$2^{-/-}$ mouse line, heterozygous constitutive PRG-$1^{-/-}$ mice were bred with LPA2-$R^{-/-}$ mice, provided by J. Chun (Contos et al., 2002).

Electron Microscopy. For ultrastructural analysis, immunogold pre-embedding labeling was performed as described previously ((Lujan et al., 1997) (Krauss et al., 2007)). Briefly, brains were perfused with 4% paraformaldehyde, 0.05% glutaraldehyde and 15% (v/v) saturated picric acid made up in 0.1 M phosphate buffer (PB, pH 7.4), and cut with a vibratome. Free-floating sections were incubated in 10% normal donkey serum (NDS) diluted in Tris buffered saline (TBS) for 1 h at room temperature. Sections were then incubated for 36 h with the primary antibody at a dilution determined by light microscopy (see above) in TBS containing 1% NDS. After several washes in TBS, sections were incubated overnight with the secondary 1.4 nm gold coupled antibody (Nanoprobes Inc., Stony Brook, NY) raised in goat, followed by silver enhancement of the gold particles with a HQ Silver kit (Nanoprobes Inc., Stony Brook, NY). Following immunogold visualization, sections were transferred to 0.1 M PB, postfixed for 30 min with 1% osmium tetroxide in 0.1 M PB, and washed several times in PB. Finally, sections were dehydrated in a graded series of ethanol for 10 min each including block staining with 2% uranyl acetate (Serva, Heidelberg, Germany) in 70% ethanol, and flat embedded in Araldite CY212 (Serva). Thin silver sections were contrasted with uranyl

acetate and lead citrate and analyzed with a LEO 912 electron microscope equipped with a slow scan digital camera (Proscan 1K) microscope.

In-vivo experiments

All experimental procedures described below were carried out in accordance with the European Communities Council Directive regarding care and use of animals for experimental procedures and were approved by Landesuntersuchungsamt Koblenz, Germany.

In utero Electroporation and expression plasmids for IUE. The in utero electroporation experiments were carried out as described (Prozorovski et al., 2008; Trimbuch et al., 2009), 2009), in accordance with a protocol approved by the local animal welfare committee. Using in utero electroporation, PRG-1 could be deleted in conditional or re-expressed in constitutive PRG-1 KO mice in a subset of cells. For in utero electroporation plasmids were prepared at 4 µg/µl by using the EndoFree Plasmid Kit (Qiagen). Timed-pregnant mice at E15-E16 (post coitum) were anesthetized with a Ketamin-Xylazinmix (Ketamine 10mg/ml; Xylazine 1mg/ml). The uterine horns were exposed and two of the pubs were randomly chosen for injecting plasmids. The DNA solution (1-1.5 µl/embryo) was injected through the uterine wall into the lateral ventricle by pulled glass capillaries (World Precision Instruments, Sarasota, USA). Electric pulses were delivered to embryos by holding the injected brain through the uterine wall with forcep-type electrodes (CUY650P5) connected to a square–pulse generator (CUY 21 Edit, Unique Medical Imada, Miyagi, Japan). Five (5) 38-V pulses of 50 ms were applied at 950 ms intervals. The uterine horns were carefully put back into the abdominal cavity before the muscle wall and skin were stitched.

The plasmids pCAG-mPRG1 and pCAG-Cre were constructed by cloning the corresponding coding frame into the MCS of a pCAG-IRES-EGFP vector (Kawauchi et al., 2003). The pCAG–PRG1R346T vector was constructed as described (Vogt et al., 2016). For in utero electroporation 16 plasmids were prepared at 4 µg/µl by using the EndoFree Plasmid Kit (Qiagen). Timepregnant mice at E15-E16 (post coitum) were anesthetized with a Ketamin-Xylazinmix (Ketamine 10mg/ml; Xylazine 1 mg/ml). The uterine horns were exposed and two of the pubs were randomly chosen for injecting plasmids. The DNA solution (1-1.5 µl/embryo) was injected through the uterine wall into the lateral ventricle by pulled glass capillaries (World Precision Instruments, Sarasota, USA). Electric pulses were delivered to embryos by holding the injected brain through the uterine wall with forceps-type electrodes (CUY650P5) connected to a square–pulse generator (CUY 21 Edit, Unique Medical Imada, Miyagi, Japan). Five (5) 38-V pulses of 50 ms were applied at 950 ms intervals. The uterine horns

were carefully put back into the abdominal cavity before the muscle wall and skin were stitched.

Morphological analyses in WT, PRG-1$^{+/-}$ and PRG-1$^{-/-}$ animals.

For dendritic spine analysis in vivo Thy-1.2-EGFP_L21 mice were mated with PRG-1+/- mice. EGFP positive brains from WT, PRG-1$^{+/-}$ and PRG-1$^{-/-}$ were than used at the postnatal (P) ages P12, P19 and adult (>6 weeks; 3 animals per genotype and age). The first 24 h after birth were defined as P0. All mice were anesthetized (0.5% ketamin i.p.) and transcardially perfused with tyrode followed by 4% (w/v) paraformaldehyd (PFA) in 0.1 M phosphate buffer (PB). Brains were removed, postfixed overnight and sectioned horizontally with a vibratome at 50 µm thickness. For immunofluorescence stainings, brain slices were permeabilized with 0.2 % Triton, blocked with 10% normal goat serum and incubated with anti VGlut-1 antibody (1:2000, Synaptic Systems) or active ITGB1 (1:200, R&D Systems) over night. Subsequently, brain slices were washed and incubated with a secondary goat anti mouse Alexa 568 antibody. Hippocampal sections were mounted on glass slides and embedded with Prolong Gold. Animals with successfully electroporated brains were processed equally in the third week of life.

Morris Water Maze

For MWM, male age matched mice were tested from 3 month onward. All experimental procedures were carried out in accordance with the European Communities Council Directive regarding care and use of animals for experimental procedures and were approved by Landesuntersuchungsamt Koblenz, Germany.

Spatial learning and memory were tested by the Morris water maze hidden platform task using the same maze and protocol as described (Postina et al., 2004). Briefly, the platform was positioned in the same quadrant for days 1 to four and the animals were released from four different positions at the pool perimeter. Mice performed four trials per day on four consecutive days with a maximal observation length of 90 s and an inter-trial interval of 90 s. If mice did not find the platform within the given time, they were gently guided to the platform. Mice were allowed to stay on the platform for 10 s. On the fifth water maze day, after removing the platform, a probe trial (60 s) was performed. Mice were automatically monitored using a computerized video system registering moving-path and duration in defined test compartments. The hardware consisted of an IBM-type AT computer combined with a video digitizer and a CCD video camera. The software used for data acquisition and analysis was EthoVision XT® release 8.0 (Noldus Information Technology, Utrecht, Netherlands).

Learning was assessed by measuring the latency to find the platform. General activity was assessed by swim speed, where mice displayed no significant differences (data not shown) and memory capabilities, which were characterized by the time mice spent searching for the platform in each quadrant.

Analysis of spine dynamics

To analyze for dynamic changes in spine density as observed by others under enriched conditions (Rampon et al., 2000), mice (EGFP-expressing (Thy1-L21) WT and PRG-1$^{-/-}$ mice) were separated after weaning in two groups. While one group was housed in large cages with three floors which were equipped with running wheels and small houses, and where fresh food and water was offered in different places to encourage for exploratory behavior, the other group was kept in isolation in a dark environment. Spine density of first order apical dendrites in the stratum radiatum (SR) of GFP-expressing CA1-neurons was analyzed at 9 weeks of age.

Supplemental References

Baron, M.K., Boeckers, T.M., Vaida, B., Faham, S., Gingery, M., Sawaya, M.R., Salyer, D., Gundelfinger, E.D., and Bowie, J.U. (2006). An architectural framework that may lie at the core of the postsynaptic density. Science *311*, 531-535.

Contos, J.J., Ishii, I., Fukushima, N., Kingsbury, M.A., Ye, X., Kawamura, S., Brown, J.H., and Chun, J. (2002). Characterization of lpa(2) (Edg4) and lpa(1)/lpa(2) (Edg2/Edg4) lysophosphatidic acid receptor knockout mice: signaling deficits without obvious phenotypic abnormality attributable to lpa(2). Molecular and cellular biology *22*, 6921-6929.

Distler, U., Schmeisser, M.J., Pelosi, A., Reim, D., Kuharev, J., Weiczner, R., Baumgart, J., Boeckers, T.M., Nitsch, R., Vogt, J.*, et al.* (2014). In-depth protein profiling of the postsynaptic density from mouse hippocampus using data-independent acquisition proteomics. Proteomics *14*, 2607-2613.

Fan, W. (2013). Group I metabotropic glutamate receptors modulate late phase long-term potentiation in hippocampal CA1 pyramidal neurons: comparison of apical and basal dendrites. Neuroscience letters *553*, 132-137.

Geromanos, S.J., Vissers, J.P., Silva, J.C., Dorschel, C.A., Li, G.Z., Gorenstein, M.V., Bateman, R.H., and Langridge, J.I. (2009). The detection, correlation, and comparison of peptide precursor and product ions from data independent LC-MS with data dependant LC-MS/MS. Proteomics *9*, 1683-1695.

Kawauchi, T., Chihama, K., Nabeshima, Y., and Hoshino, M. (2003). The in vivo roles of STEF/Tiam1, Rac1 and JNK in cortical neuronal migration. The EMBO journal *22*, 4190-4201.

Krauss, M., Weiss, T., Langnaese, K., Richter, K., Kowski, A., Veh, R.W., and Laube, G. (2007). Cellular and subcellular rat brain spermidine synthase expression patterns suggest region-specific roles for polyamines, including cerebellar pre-synaptic function. Journal of neurochemistry *103*, 679-693.

Lujan, R., Roberts, J.D., Shigemoto, R., Ohishi, H., and Somogyi, P. (1997). Differential plasma membrane distribution of metabotropic glutamate receptors mGluR1 alpha, mGluR2 and mGluR5, relative to neurotransmitter release sites. J Chem Neuroanat *13*, 219-241.

Patzig, J., Jahn, O., Tenzer, S., Wichert, S.P., de Monasterio-Schrader, P., Rosfa, S., Kuharev, J., Yan, K., Bormuth, I., Bremer, J.*, et al.* (2011). Quantitative and integrative proteome analysis of peripheral nerve myelin identifies novel myelin proteins and candidate neuropathy loci. J Neurosci *31*, 16369-16386.

Postina, R., Schroeder, A., Dewachter, I., Bohl, J., Schmitt, U., Kojro, E., Prinzen, C., Endres, K., Hiemke, C., Blessing, M.*, et al.* (2004). A disintegrin-metalloproteinase prevents amyloid plaque

formation and hippocampal defects in an Alzheimer disease mouse model. The Journal of clinical investigation *113*, 1456-1464.
Prozorovski, T., Schulze-Topphoff, U., Glumm, R., Baumgart, J., Schroter, F., Ninnemann, O., Siegert, E., Bendix, I., Brustle, O., Nitsch, R.*, et al.* (2008). Sirt1 contributes critically to the redox-dependent fate of neural progenitors. Nature cell biology *10*, 385-394.
Rampon, C., Tang, Y.P., Goodhouse, J., Shimizu, E., Kyin, M., and Tsien, J.Z. (2000). Enrichment induces structural changes and recovery from nonspatial memory deficits in CA1 NMDAR1-knockout mice. Nature neuroscience *3*, 238-244.
Schmeisser, M.J., Ey, E., Wegener, S., Bockmann, J., Stempel, A.V., Kuebler, A., Janssen, A.L., Udvardi, P.T., Shiban, E., Spilker, C.*, et al.* (2012). Autistic-like behaviours and hyperactivity in mice lacking ProSAP1/Shank2. Nature *486*, 256-260.
Sholl, D.A. (1953). Dendritic organization in the neurons of the visual and motor cortices of the cat. J Anat *87*, 387-406.
Silva, J.C., Denny, R., Dorschel, C.A., Gorenstein, M., Kass, I.J., Li, G.Z., McKenna, T., Nold, M.J., Richardson, K., Young, P.*, et al.* (2005). Quantitative proteomic analysis by accurate mass retention time pairs. Anal Chem *77*, 2187-2200.
Tenzer, S., Docter, D., Rosfa, S., Wlodarski, A., Kuharev, J., Rekik, A., Knauer, S.K., Bantz, C., Nawroth, T., Bier, C.*, et al.* (2011). Nanoparticle size is a critical physicochemical determinant of the human blood plasma corona: a comprehensive quantitative proteomic analysis. ACS nano *5*, 7155-7167.
Tokumitsu, H., Hatano, N., Tsuchiya, M., Yurimoto, S., Fujimoto, T., Ohara, N., Kobayashi, R., and Sakagami, H. (2010). Identification and characterization of PRG-1 as a neuronal calmodulin-binding protein. Biochem J *431*, 81-91.
Trimbuch, T., Beed, P., Vogt, J., Schuchmann, S., Maier, N., Kintscher, M., Breustedt, J., Schuelke, M., Streu, N., Kieselmann, O.*, et al.* (2009). Synaptic PRG-1 modulates excitatory transmission via lipid phosphate-mediated signaling. Cell *138*, 1222-1235.
Vogt, J., Glumm, R., Schluter, L., Schmitz, D., Rost, B.R., Streu, N., Rister, B., Suman Bharathi, B., Gagiannis, D., Hildebrandt, H.*, et al.* (2012). Homeostatic regulation of NCAM polysialylation is critical for correct synaptic targeting. Cellular and molecular life sciences : CMLS *69*, 1179-1191.
Vogt, J., Yang, J.W., Mobascher, A., Cheng, J., Li, Y., Liu, X., Baumgart, J., Thalman, C., Kirischuk, S., Unichenko, P.*, et al.* (2016). Molecular cause and functional impact of altered synaptic lipid signaling due to a prg-1 gene SNP. EMBO molecular medicine.
Wisniewski, J.R., Zougman, A., Nagaraj, N., and Mann, M. (2009). Universal sample preparation method for proteome analysis. Nat Methods *6*, 359-362.